GENERATION OF SYNTHETIC EARTHQUAKE MOTIONS AND THEIR APPLICATION TO DYNAMIC RESPONSE ANALYSES

by

Tetsuo Kubo[I] and Norio Suzuki[II]

SYNOPSIS

Through the relation of Fourier transformation, two types of stochastic modeling of earthquake motion are introduced. By use of these two modelings, twenty samples of synthetic motion, in each case, are generated simulating a recorded earthquake motion. Upon these synthetic motions, characteristics of waveform such as the cumulative energy distribution (the integration of square acceleration), the maximum elastic response and the maximum inelastic response are evaluated. The results are compared with those obtained from the recorded motion and the correlation of dynamic response properties between the recorded motion and the synthetic motion are determined.

INTRODUCTION

To determine an earthquake excitation when carrying out dynamic aseismic design of a structural system, two alternatives could be given. One is to use a waveform of motion, and the other is to use a design spectral diagram such as that proposed in literatures [1,2]. The former can further be divided into the following two procedures.

One is to determine a waveform either by real strong motion waveforms such as those made at El Centro, California during the Imperial Valley earthquake of 1940 and at Hachinohe Harbour, Japan during the Tokachi-Oki earthquake of 1968 with general consideration upon such as subsoil conditions, or by real waveforms of small- or moderate-size earthquakes made at the site with an appropriate scaling. Since, however, earthquake motions, even recorded at the same location, have often yielded quite dissimilar characteristics, this approach is subject to question "Could the specific motion of a past earthquake obtained at the specific location be representative of a future earthquake motion at a certain location?"

The other is to determine a waveform by a stochastic process having appropriate properties in a statistical sense. With recent development of seismological researches, determining source mechanisms and physical properties of wave propagation path, a time trace of an earthquake motion can be calculated. However, recognizing complexity and irregularity in the initiation of seismic wave and its propagation path, stochastic modeling is a realistic and feasible approach for engineering practice.

I Research Engineer, Building Research Institute, Ministry of Construction, Japanese Government, Tsukuba New Town for Research and Education, Ibaraki, Japan.

II Graduate Student, University of Tokyo, Tokyo, Japan.

GENERATION OF SYNTHETIC EARTHQUAKE MOTIONS

A suitably integrable time function f(t) uniquely corresponds to its Fourier transform. Conversely, a Fourier transform defines the corresponding time function through

$$F(\omega) = \int_{-\infty}^{\infty} f(t)\, e^{-j\omega t}\, dt \qquad (1)$$

$$f(t) = \frac{1}{2\pi} \int_{-\infty}^{\infty} F(\omega)\, e^{j\omega t}\, d\omega \qquad (2)$$

Fourier transform $F(\omega)$ of $f(t)$ in Eq. (1) can be expressed as follows;

$$F(\omega) = A(\omega) \exp [-j\Phi(\omega)] \qquad (3)$$

where

$$A(\omega) = |F(\omega)| \qquad (4)$$

$$\Phi(\omega) = -\tan^{-1} [\mathrm{Im}[F(\omega)]/[\mathrm{Re}[F(\omega)]] \qquad (5)$$

are called a Fourier amplitude spectral function and a Fourier phase spectral function, respectively. Equations (1) through (5) indicate that time function $f(t)$ and a pair of spectral functions $A(\omega)$ and $\Phi(\omega)$ define uniquely each other.

Provided that $f(t)$ is a real function and is defined in discrete form within the finite interval of 0 and T_D, Eq. (2) can be written by

$$f(t) = \sum_{n=0}^{N/2} a_n \cos(\omega_n t - \phi_n) \qquad (6)$$

where

$$a_n = \begin{cases} \frac{\Delta\omega}{2\pi} A_n & (n=0 \text{ or } n=N/2) \\ \frac{\Delta\omega}{\pi} A_n & (\text{otherwise}) \end{cases}$$

$$A_n = A(\omega_n), \quad \phi_n = \Phi(\omega_n) \qquad (7)$$

$$\omega_n = n\Delta\omega = n\frac{2\pi}{T_D}, \text{ and } N = \frac{T_D}{\Delta t}$$

in which Δt designates equi-time-spacing of $f(t)$.

Let Fourier spectral functions obtained from a recorded earthquake accelerogram $f_o(t)$ be denoted by $A_o(\omega)$ and $\Phi_o(\omega)$, respectively. The following two stochastic modelings of synthetic earthquake motions are introduced.

One, named the Type I Modeling, is to generate a Fourier phase function by analysis of a real earthquake motion and to determine Fourier amplitudes by uniformly distributed random numbers, i.e.

$$g_i(t) = \sum_{n=0}^{N/2} a_{in} \cos(\omega_n t - \phi_{on}) \quad (i=1,2,\cdots) \qquad (8)$$

where i denotes the i-th individual member from the ensemble and a_{in}'s are random numbers distributed uniformly in the interval of 0 and 1.

The other, the Type II Modeling, is to define a Fourier amplitude function from analysis of a real motion giving random angles uniformly distributed over the range between 0 and 2π to a Fourier phase function;

$$g_i(t) = \sum_{n=0}^{N/2} a_{on} \cos(\omega_n t - \phi_{in}) \quad (i=1,2,\cdots) \qquad (9)$$

in which random phase angles ϕ_{in}'s are distributed uniformly over the range $0 \leq \phi_{in} < 2\pi$.

SYNTHETIC EARTHQUAKE MOTIONS

Type I Modeling Both mathematical expectation and autocorrelation function are given as function of time [3]. The processes defined by Eq. (8) show nonstationarity.

Random amplitudes in Eq. (8) take values in the range $0 \leq a_{in} < 1$. When compared with a recorded motion, the generated waveform should be appropriately scaled. Among many earthquake intensity scales proposed, the scale introduced by Arias [4] is accepted in this study. Setting the intensity scale of a synthetic motion equal to that of the recorded motion, waveform of a synthetic earthquake motion $f_i(t)$ is yielded through

$$f_i(t) = c_i \, g_i(t) \qquad (10)$$

where c_i is a scaling factor obtained from

$$c_i = \sqrt{\int_o^{T_D} f_o^{\,2}(t)\, dt \;/\; \int_o^{T_D} g_i^{\,2}(t)\, dt} \qquad (11)$$

in which $f_o(t)$ represents the real earthquake accelerogram.

Type II Modeling Mathematical expectation and autocorrelation function are both given time invariant. Average over time of any member from the ensemble equals its corresponding average across the ensemble [3]. The process is, in addition to being stationary, ergodic.

Since the process is stationary, it should be multiplied by an appropriate deterministic time function to take adequate rise-up and decaying of intensity during shaking. To quantify the variation of intensity of waveform, let the following integral be introduced

$$E_i(t) = \int_o^t f_i^{\,2}(s)\, ds \qquad (12)$$

which is called the Husid plot. Suppose synthetic earthquake motion $f_i(t)$ be expressed by the product of random process $g_i(t)$ in Eq. (9) and deterministic time function $\zeta(t)$,

$$f_i(t) = \zeta(t) \, g_i(t) \qquad (13)$$

Deterministic function $\zeta(t)$ is obtained a synthetic motion to be expected to have a similar Husid plot to that of the recorded motion, thus

$$\zeta(t) = \sqrt{T_D \frac{d}{dt} \{E_o(t)/E_o(T_D)\}} \qquad (14)$$

or in a normalized form,

$$\zeta(\tau) = \sqrt{\frac{d}{d\tau} e_o(\tau)} \qquad (15)$$

where τ and e_o denote normalized time t/T_D and normalized quantity $E_o(t)/E_o(T_D)$, respectively, in which T_D designates duration of an entire record.

Intensity function $\zeta(t)$ is established as follows. In Fig. 1(a), the Husid plot for the recorded motion is shown. Divide x and y axes into m and n pieces, respectively. Connect the intersecting points in order, and approximate the curve by pieces of straight line. A deterministic function is established by a step function shown in Fig. 1(b).

Earthquake Waveform In this study, the recorded accelerogram, S00°E component at El Centro obtained during the Imperial Valley earthquake of May 18, 1940 is selected. Time trace of the real motion is shown in Fig. 2. By use of the two types of modeling, twenty samples of synthetic motion, in each case, are produced simulating the recorded motion, and their time traces are presented in Figs. 3 and 4, respectively. Common occurrence time 2.44 sec. of the peak acceleration is found for the synthetic motions while 2.12 sec. for the real motion. Statistics of the peak acceleration is summarized in Table 1.

CUMULATIVE ENERGY DISTRIBUTION

Let the energy contained in waveform $f_i(s)$ during interval $0 \leq s < t$ be defined by

$$E_i(t) = \int_o^t f_i^2(s)\, ds \qquad (16)$$

thus by the integration of square acceleration. Normalize the quantity and obtain the so-called "normalized cumulative energy function" for the purpose of examining energy distribution of waveform associated with time,

$$e_i(\tau) = E_i(t)/E_i(T_D) \qquad (17)$$

where τ and E_i denote normalized time variable t/T_D and the energy of waveform defined by Eq. (16), respectively. For motions from the Type II modeling, the energy function is expected to coincide with that of the recorded motion although including certain amount of fluctuation. Examination is conducted only upon motions from the Type I modeling.

Cumulative energy functions both for the recorded motion and for the synthetic motions are presented in Fig. 5. Axes x and y represent normalized time variable τ and normalized energy e, respectively. Six curves in the figure show the cumulative energy functions for cases described as follows; the thick solid curve for that of the recorded motion, the thin solid curve for the mean value of energy functions obtained from the twenty samples of synthetic motion, two dot-dashed curves for the

mean value plus and minus ten times standard deviation obtained from the synthetic motions, and two dashed curves for maximum and minimum values obtained among the synthetic motions.

Figure 5 shows that the cumulative energy for the synthetic motions falls within quite a narrow range. Energy functions of motions from the Type I modeling reveal quite similar plots with one another. Envelope curve which specifies intensity of waveform varying with time takes a similar form not only among the synthetic motions but also to that obtained from the recorded motion.

MAXIMUM ELASTIC RESPONSES

Spectral diagrams in Figs. 6 and 7 show maximum elastic responses for motions of the selected component from both the Type I modeling and the Type II modeling, respectively. Axes x and y represent the undamped natural period of an oscillating system and the maximum pseudo velocity response with a fraction of the critical damping of 0.05 associated in the system. In these figures, the thick solid curve, the thin solid curve and two dashed curves represent the results of the maximum response obtained from the recorded motion, of the arithmetic mean over maximum responses obtained from the synthetic motions, and the maximum and the minimum of maximum responses obtained from the synthetic motions, respectively. The shaded zone shows the range where the response is given a value in the interval of the mean plus and minus one standard deviation taken across the responses obtained from the twenty samples of synthetic motion.

Type I Modeling From the correlation between the maximum pseudo velocity response and Fourier amplitude, the plot of the thin solid curve will be flat. The synthetic motions produce smaller magnitude of responses in the intermediate range of periods than the real motion. Dominant periods of motion cannot be observed included which is one of the characteristic features of earthquake motion in an engineering sense. The Type I modeling is concluded not adequate for an engineering application.

Type II Modeling Although smoothed as an arithmetic mean, the thin solid curve coincides with the thick solid curve with good agreement over the entire range of period. Response obtained from the recorded motion falls in the shaded zone representing the range between the mean value plus and minus one standard deviation taken across the synthetic motions. The twenty responses obtained from the synthetic motions associated with a certain natural period have a tendency to fall in value around the mean value. Though distribution of the responses cannot be concluded Gaussian by the chi-square goodness-of-fit test with confidential level of 50 percent, numerical analysis yields the result that a maximum response subject to a synthetic motion is not greater than the mean value plus one standard deviation with probability of 85 percent, while the corresponding probability is 84.13 percent in case of the Gaussian distribution.

MAXIMUM INELASTIC RESPONSES

Responses of a linear elastic system subject to a stochastic process can be theoretically determined by variations of statistical quantities associated with the input process. For a nonlinear inelastic system,

in general cases, one is forced to conduct a numerical analysis. In this case, input excitation is essentially made explicitly by a waveform of motion. Upon the synthetic motions produced by the Type II modeling, maximum inelastic responses are evaluated and are compared with those obtained from the recorded motion.

In Fig. 8, a schematic rule of the Degrading Tri-Linear hysteresis employed in this study is described, which is one of representative rules for a reinforced concrete system. Cracking capacity k_c and yielding capacity k_y are 100 gal and 300 gal, respectively, and the ratio of the second stiffness ω_2^2 to the initial one ω_1^2 is 1/4. Multiplying amplitudes of waveform by scaling factors 0.878 and 1.171 so as the resulting peak acceleration of the real motion k_g to be 300 gal and 400 gal, the maximum displacement responses are evaluated both for the recorded motion and for the synthetic motions. Figures 9(a) and 9(b) present the results for k_g to be 300 gal and 400 gal, respectively. The legends such as the thick solid curve, the thin solid curve, the dashed curves and the shaded zone in these figures are identically similar to those in figures representing the results of elastic responses.

Observation upon these figures leads to the evidence that the response obtained from the recorded motion and the mean value over responses from the synthetic motions coincide well with each other over the entire range of periods. Response obtained from the recorded motion usually falls in the shaded zone. On an average, in sixteen or seventeen cases out of twenty, responses obtained from the synthetic motions have values not greater than the mean value plus one standard deviation taken across the responses obtained from the synthetic motions.

CONCLUDING STATEMENTS

Through the property of Fourier transforms, two types of stochastic modeling of synthetic earthquake motion are introduced. Synthetic earthquake motions are generated simulating a certain selected real motion. In an attempt to make engineering use of synthetic motions for structural design, characteristics of waveform such as the cumulative energy distribution, the maximum elastic response and the maximum inelastic response are evaluated and are compared from a statistical viewpoint with those obtained from the recorded motion. Dynamic properties of motions produced by these two modelings are summarized as follows.

Type I Modeling The Type I motions are nonstationary in intensity with time, and reveal quite a similar cumulative energy distribution with one another. General plot of an envelope intensity function obtained from the synthetic motions has similarity to that from the recorded motion. In the maximum elastic response analysis, certain dominant periods included in the real motion which is one of the characteristic features of earthquake motion cannot be synthesized.

Type II Modeling The mean value of responses both in elastic analysis and in inelastic analysis coincides with the response obtained from the recorded motion with good agreement over the entire range of natural periods of an oscillating system. In both analyses, the maximum response obtained from an individual member from the synthetic motions takes the

value not greater than the mean value plus one standard deviation obtained by statistical analysis over the synthetic motions with probability of higher than 80 percent.

Although motions generated by the Type I modeling are concluded not adequate for an engineering application, they reveal quite a specific feature in intensity with time. It is required that a mathematical modeling of synthetic earthquake motion will be developed with consideration upon phase angles of waveform to produce more realistic synthetic motions for an extensive application to engineering practice.

ACKNOWLEDGMENT

For other components of real earthquake accelerograms, similar analysis and observation has been carried out [3,5]. The authors are indebted to Professors H. Umemura and H. Aoyama, University of Tokyo, Tokyo for their continuous guidance and encouragement through the course of study.

REFERENCES

[1] Newmark, N. M. and E. Rosenblueth, "Fundamentals of Earthquake Engineering," Prentice-Hall, Inc., 1971.

[2] Newmark, N. M., J. A. Blume and K. K. Kapur, "Seismic Design Spectra for Nuclear Power Plants," Jour. Power Div., ASCE, Vol. 99, No. PO2, pp. 287-303 (1973).

[3] Kubo, T. and N. Suzuki, "Simulation of Earthquake Ground Motion and Its Application to Response Analysis," Trans. Archi. Inst. Japan, No. 275, pp. 33-43, (1979) (in Japanese).

[4] Arias, A., "A Measure of Earthquake Intensity," in "Seismic Design for Nuclear Power Plants," ed. R. J. Hansen, MIT Press, pp. 438-483, 1970.

[5] Kubo, T., and N. Suzuki, "Simulation of Earthquake Ground Motion and Its Application to Dynamic Response Analysis," Proc. Fifth Japan Earthq. Engng Symp., pp. 89-96, November 1978.

TABLE 1 STATISTICS OF THE PEAK ACCELERATION

Recorded (gal)	Synthetic					
	Model	Maximum (gal)	Minimum (gal)	Mean (gal)	Standard Deviation (gal)	Coefficient of Variation
341.7	I	559.48	446.39	501.93	30.63	0.063
	II	494.37	245.62	316.14	59.35	0.188

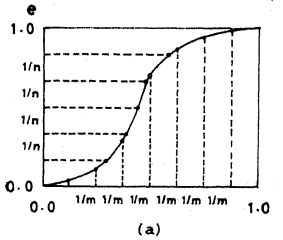

(a)

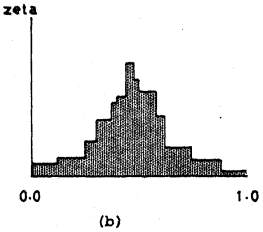

(b)

Fig. 1 Deterministic intensity function.

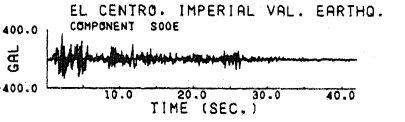

Fig. 2 Time trace of the recorded motion, the S00°E component, El Centro.

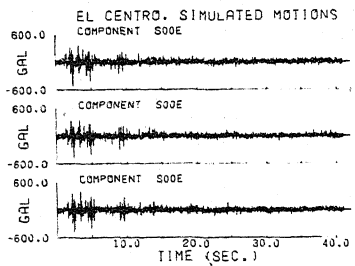

Fig. 3 Time traces of the synthetic motions from the Type I Modeling, the S00°E component, El Centro.

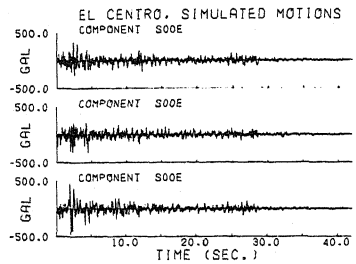

Fig. 4 Time traces of the synthetic motions from the Type II Modeling, the S00°E component, El Centro.

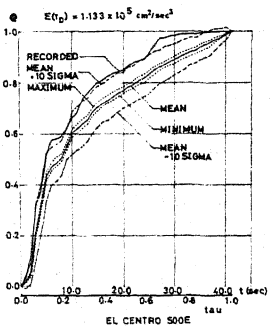

Fig. 5 Cumulative energy distribution for the S00°E component, El Centro.

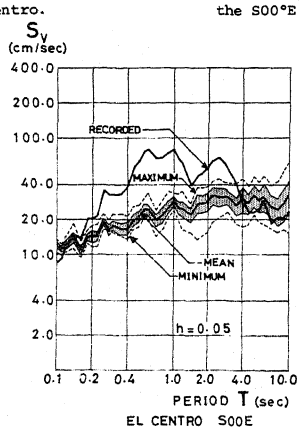

Fig. 6 Elastic response spectra for the recorded and the synthetic motions from the Type I Modeling, the S00°E component, El Centro.

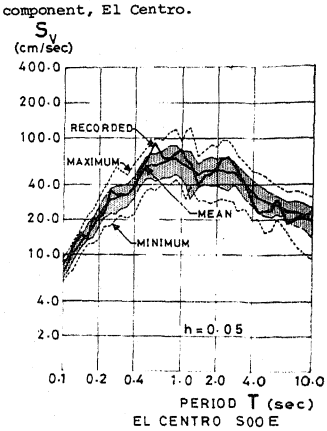

Fig. 7 Elastic response spectra for the recorded and the synthetic motions from the Type II Modeling, the S00°E component, El Centro.

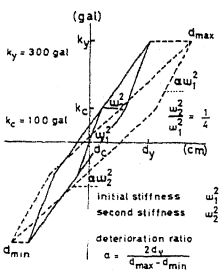

Fig. 8 Hysteresis rule of the Degrading Tri-Linear model.

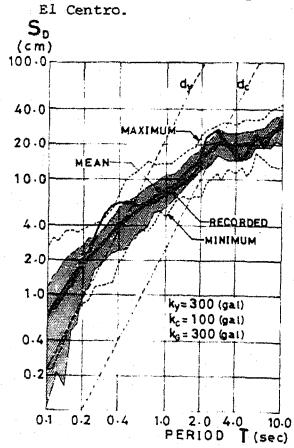

(a) k_g = 300 gal

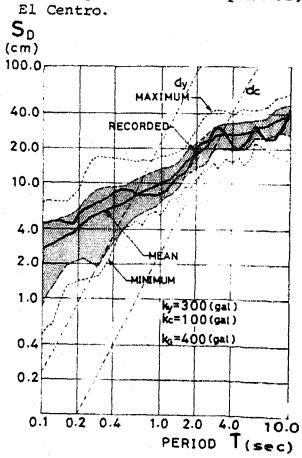

(b) k_g = 400 gal

Fig. 9 Inelastic response spectra for the recorded and the synthetic motions from the Type II Modeling, the S00°E component, El Centro.